Crustal structure and deformation across a mature slab tear zone: the case of southern Tyrrhenian Subduction (Italy)

Irene Bianchi 1, Francesco Pio Lucente 2, Massimo Di Bona 2, Aladino Govoni 2 and Nicola Piana Agostinetti 3

1 Institut für Meteorologie und Geophysik, Universität Wien, Vienna, Austria

2 Istituto Nazionale di Geofisica e Vulcanologia, Centro Nazionale Terremoti, Rome, Italy

3 Geophysics Section, School of Cosmic Physics, Dublin Institute for Advanced Studies, Dublin, Ireland

Corresponding author: Irene Bianchi (irene.bianchi@univie.ac.at)

Key Points:

- The seismic structure of the crust across the deformation zone associated with the tear in the Ionian slab is investigated, between Southern Calabria and Sicily (Italy)
- The isotropic S-wave velocities profiles show the clear differences at the boundaries of the deformation zone, pointing out the different origin for the crust in the two regions
- Anisotropy at mid-crustal depth develops both in Sicily and in Southern Calabria, with identical geometrical parameters, and shows connections with the deformation due to the differential movement of the retreating slab

Abstract

We compute S-velocity profiles of the crust across the Messina strait (Italy), the tear zone at the southern end of the Ionian subduction zone. Separating Sicily from Calabria, the Messina Strait hosted some of the strongest earthquakes to ever occur in Italy. Here, the motion of the Ionian slab with respect to Sicily creates a complex tectonic setting characterized by lithospheric tearing. We show velocity models of the crust, computed from teleseismic receiver function inversion, outlining the differences between Sicily and Calabria. Strong

This article has been accepted for publication and undergone full peer review but has not been through the copyediting, typesetting, pagination and proofreading process which may lead to differences between this version and the Version of Record. Please cite this article as doi: 10.1002/2016GL070978

deformation across the Messina Strait between 10-15 and 30 km depth is expressed by strong anisotropy (up to 10%), developed in a ductile shear zone of the crust. The top of these ductile, weaker layers could limit the depth-extent of future ruptures.

1. Introduction

Subduction causes tectonic deformation in the lithospheric plates and in the ambient mantle. Along the southeastern corner of the Tyrrhenian Basin, a deep seismic zone indicates that the Ionian plate dips to the northwest beneath the Calabrian Arc (Figure 1). Here, some of the most destructive earthquakes have occurred [*Rovida et al.,* 2011]. Seismic tomography provides evidence for a 200-300 km-wide, arched, high velocity anomaly dipping 70–80° below Calabria into the transition zone [e.g., *Lucente et al.,* 1999; *Chiarabba et al.,* 2008]. Its descent is accompanied by an eastward slab rollback [*Malinverno and Ryan,* 1986; Faccenna *et al.,* 2001; *Rosenbaum and Lister*, 2004]. The slab is continuous beneath southern Calabria only [e.g. *Wortel and Spakman,* 2000; *Calò et al.,* 2009; *Neri et al.,* 2009], while slab tear at the edges of the subduction zone may explain the absence of deep seismicity underneath Sicily and southern Apennines [*Orecchio et al.,* 2014; *Chiarabba et al.,* 2016]. Due to the different subduction rates between the Calabrian arc (ongoing), and the tectonically locked Sicily, a complex transfer zone at the boundary between the two kinematic domains has developed beneath the Messina Strait. In case of a rapid retreating slab, the lateral edges host a "Subduction-Transform Edge Propagator" (STEP) faults in the subducting slab [e.g. *Barreca et al.*, 2016]. While STEP faults have been worldwide studied, deformation in the overriding plate, especially at the edges, is poorly understood. We constrain the structure of the Southern Tyrrhenian subduction zone at its southern edge by receiver function (RF) analysis to gain insight into the deformation behavior there.

We compute RF from 3000 teleseismic P-waves recorded at 10 temporary stations operating during the "Messina 1908–2008" research project [*Margheriti,* 2008] (Figure 1) and at 3 permanent stations from the Italian National Seismic Network of INGV. The trans-dimensional Markov chain Monte Carlo algorithm by *Piana Agostinetti and Malinverno* [2010] has been applied to derive the crustal and uppermost mantle structure below each station. We make a harmonic analysis of the RF data-set [*Bianchi et al.,* 2008; *Bianchi et al.,* 2010] to infer the presence of anisotropic layers at crustal depth and deformation.

2 Data and Methods

2.1 RF data-set

To obtain a RF data set for the 13 broadband seismic stations, we selected teleseismic events with magnitude Mb ≥ 5.5 and epicentral distance (Δ) in the range of 30° - 105°. The waveforms are selected using a signal-to-noise (S/N) ratio criterion. While for the 3 permanent stations we have available several years of recordings, hence we can optimize the selection of teleseisms, the data sets at the temporary stations are inevitably of lower quality (less complete backazimuthal coverage, lower signal-to-noise ratio).

For the 10 temporary stations, the final dataset includes 716 3-component records, with a minimum of 57 and a maximum of 96 records for single station (Figure 2b, and S1-S12).

We obtain the RF by deconvolving the vertical from the horizontal components to the RTZ (radial-transverse-vertical) reference system using the frequency-domain approach by *Di Bona* [1998].

To increase the S/N ratio the RF have been stacked within bins which are 20° wide in back azimuth (baz) and 40° wide in Δ, and are computed every 10° in baz, each sharing with the adjacent 50% of its traces. A representative set of RF as a function of back-azimuth is displayed in Figure 2a for station MTTG, time 0 corresponds to the arrival of the direct P-wave, and time is the relative delay time of the Ps converted phases with respect to the P-direct. The P-wave (apparent) offset is due to the presence of shallow dipping interfaces (*Cassidy*, 1992, and Figure S13).

2.2 Harmonic analysis

Most of the stations used in this study show RF transverse components with non-negligible amplitude (Figure 2a and S1-S12a), hence possessing a complex structure at depth (as is expected in such a geodynamical context), such as dipping discontinuities or anisotropy [*Levin and Park,* 1998]. Therefore, we apply a technique that allows the separation of the backazimuth harmonics of the R- and T-RFs (radial and transverse RF, respectively) data set as a function of the incoming wave-field direction [*Bianchi et al.,* 2008, and references therein]; after being computed by *Di Bona*'s (1998) method we apply the harmonic decomposition following the method described in *Bianchi et al.* [2010]. Harmonic decomposition separates the "isotropic contribution", on the k=0 harmonics, from the contribution given by anisotropy with plunging symmetry axis, and/or dipping interfaces on the k=1, these two indeed generating a two-lobed polarity reversal in the backazimuthal sweep; anisotropy with horizontal axis is instead represented by the k=2 term of the harmonic

decomposition, due to the fact that anisotropy with a symmetry axis in the horizontal plane generates a four lobed polarity reversal in the backazimuthal sweep (Figure 2b). Herein after, the term "isotropic contribution" indicates the P-to-S energy converted at "isotropic interfaces", i.e. a discontinuity where the bulk seismic velocity varies on the two sides. At the same time, we refer to "anisotropic/dipping contribution" to the P-to-S energy converted at the top or bottom of an anisotropic layer, or at a planar dipping interface separating any kind of couple of layers, either isotropic or anisotropic [*Bianchi et al.,* 2010]. Due to the limited energy on the k=2 harmonics for our RF data sets (Figure 2b, S1-S2b), in the following we limit our analysis to the first two harmonics (k=0 and k=1) this means that little or no anisotropy with horizontal symmetry axis is present in the area, at the depth that we are exploring. Uncertainties on the k=0 and k=1 harmonics are retrieved using a bootstrap approach, i.e. repeating one hundred times the computation of k=0 and k=1 harmonics using randomly resampled RF dataset [*Piana Agostinetti and Miller,* 2014]. The k=0 harmonics can be inverted to reconstruct the 1D S-wave velocity (Vs) profiles beneath an isolated seismic station, while information about the presence and the position at depth of anisotropic layers and dipping interfaces can be extracted from the k=1 harmonics of the RF data-set.

2.3 1D Velocity profiles

To obtain the 1D Vs profile for each of the 13 seismic stations, we apply a trans-dimensional Monte Carlo method for the inversion of RF data developed by *Piana Agostinetti and Malinverno* [2010]. The k=0 harmonics, together with their estimated standard deviation (Figure 2c, and S1-S12c), are used as input data to solve the inverse problem and gain inferences on the isotropic structure. The Vs model below a seismic station is retrieved by sampling the *a priori* parameter space, and retrieving a posterior probability distribution by the application of the so called reversible jump Markov chain Monte Carlo (RjMCMC). The *a priori* probability distributions of the S velocity and Vp/Vs are considered Gaussian (Table S3). In the *a priori* information, the Vp/Vs is set constant to 1.75 with 0.05 standard deviation from top to bottom, while for the Vs larger velocity variations are allowed at shallow depth (Table S3).

The number of interfaces can vary between 1 and 30; the maximum depth of the interfaces is fixed to 60 km, being 30 s the length of the RRF used in the inversion. The likelihood function between observed and synthetic RF is computed using a full covariance matrix for the errors.

The RjMCMC method is first used to sample about 100,000 models for one Markov chain. We obtain an ensemble of 10^7 velocity models (for each single station) by running 100 RjMCMC parallel computations; out of the 10^7 models, we calculate the posterior probability distribution (PPD) [as in *Piana Agostinetti and Malinverno*, 2010]. The output of the RjMCMC search gives the Vs PPD at depth (Figure 2d), and the distribution of seismic interfaces at depth (Figure 2e) together with the indication of the number of layers constituting the model (Figure 2f).

The application of the technique is shown in Figure 2c-f for the k=0 harmonic obtained at station MTTG. The posterior S-wave depth distribution is used to retrieve a mean Vs model and to assess the uncertainties (Figure 2d). The k=0 harmonic is compared with the synthetic RRF in Figure 2c, predicted RF were obtained using the code developed by *Shibutani et al.* [1996]. The full representation of the RjMCMC search results obtained at all stations is given in Figures S1-S12.

As previously stated, temporary stations yield lower quality data with respect to permanent stations, not allowing inverting the RFs data for the three-dimensional structure. Therefore, at the 10 temporary stations, we limit the analysis to the determination of the 1D Vs profile.

2.4 3D Velocity profiles

At the three permanent stations we perform a search of the 3D characteristics of the subsurface structure, by fitting the k=1 term of the harmonic decomposition. The employed RjMCMC algorithm is to date not able to resolve the non-isotropic characteristics of the media; we use the Neighborhood Algorithm (NA) [*Sambridge*, 1999] in order to constrain dipping interfaces and anisotropy at depth.

We divide the RjMCMC retrieved Vs model into a layered model with uniform velocity in each layer. We assign 3D values to the layers to apply the NA; in particular we assign to the middle crustal layers P- and S- anisotropy values ranging between 0 and 10%, (Table S1). In the NA search, the space is divided into Voronoi cells that sample the multidimensional parameter space, and lead the search to an ensemble of models that fit the data. Initially 1,500 samples are created randomly, and then 1,000 new samples are extracted from the 500 cells holding the lowest misfit to the data. After 400 iterations we obtain 401,500 models for each station, among these the best-fitting model is considered as representative of the whole model ensemble. The code RAYSUM [*Frederiksen and Bostock*, 2000] is used to compute the synthetic seismograms, simulating the propagation of a seismic wave through both dipping interfaces and anisotropic layers. Multiple phases from the shallowest layer,

generally the largest in amplitude due to the high impedance contrast between sediments and bedrock, have been accounted in order to ensure that they are not interpreted as primary conversions. Anisotropy is considered as hexagonal with a fast or slow symmetry axis [*Levin and Park*, 1998]. We set P and S anisotropic parameters as equal in order to lighten the computation load. We consider the signal arriving on the T component at smaller delay times as originated by dipping interfaces, and signal arriving at larger delay time (larger than 2 s), as originated by anisotropic layers at depth. A dipping interface at depth requires a large inclination angle in order to produce amplitudes as large as those due to anisotropic layers with average or small anisotropy [*Lucente et al.,* 2005; *Bianchi et al.,* 2008]. Although the Ionian slab dips of 70° further to the NW, beneath the Southern Tyrrhenian sea, as seen by the distribution of intermediate-depth events, a high angle structure (dipping >45°) is unexpected at middle-to-lower crustal depth in the study area. Indeed the Ionian plate shows a monoclinal inclination of 9-12 degrees [*Cassinis et al*., 2003], and the dip angle increases beneath Calabria, reaching no more than 20 degrees [*Piana Agostinetti et al.,* 2009]. Therefore we do not expect to encounter highly dipping structures beneath Calabria, and although we might have modelled the later pulses by means of dipping interfaces, a higher dip angle would have been needed, contrasting the regional monoclinal inclination.

For the definition of the parameter space we consider a fast anisotropic axis. A fast-symmetry-axis can be representative of anisotropy in amphibolites, generated by crystallographic fabric of its constituent minerals (hornblende, *Meissner et al*., 2006). While the choice of a fast-axis is somehow subjective and a slow-axis can also be representative of anisotropic materials at the same crustal depth (e.g. *Porter et al.,* 2011), it does not affect the inferences on the symmetry axis direction in anisotropic materials [*Bianchi et al.,* 2008]. The comparison between synthetic and observed terms of the first-order harmonic (k=1), are displayed in Table S2, together with the best-fitting velocity models, and synthetic RF relative to the models in Table S2 are displayed in Figures S13, S14 and S15 along the backazimuthal sweep.

3. Results

3.1 1D Structure

The 1D velocity profiles, shown for all the 13 stations (Figures 2d, S1-S12d), have been gathered based on the stations geographical location following the Calabrian arcuate shape; as result we obtain four average velocity profiles, representative of different areas (Figure 3a-h).

Stations ME03 and CEL are located in Tyrrhenian Calabria (TC), both are sited along the coast on the border of the Tyrrhenian sea, CEL and ME03 are located on the sedimentary deposits at the foothill of the Apennines; characteristics of the velocity models retrieved for these two stations, are the occurrence of impedance contrasts at shallow depths (10 and 20 km depth) (Figure 3a,b) and a slow velocity gradient down to the Moho interface estimated being deeper than 40 km depth. ME05, ME10, MRCB are located in Central Calabria on the Calabrian Nappes, constituted by pre-alpine basement, the stations belonging to this group show the most heterogeneous velocity models among all inspected sites; strong impedance contrasts are present in the first 15 km (Figure 3d,e), and at 25 km depth, the Moho is at about 37 km; the mean velocity models show a decrease in velocity for mid-crustal layers at about 25 km. Velocity profiles retrieved for MTTG and ME09 define the structure of Ionian Calabria (IC), being located on the metamorphic rocks of the southwestern tip of Calabria. Both of them indicate a velocity decrease at about 25 km depth, and a gradient in the lower crust to the Moho at about 35 km depth (Figure 3f,g). MALI, NOV, MMME, ME15, ME01 are located in Sicily; all velocity profiles retrieved for these station have as common characteristics the lack of strong impedance contrasts, rather a constant velocity increase with depth (Figure 3i,j). Here, we identify the Moho as the maximum of the cumulative histogram for the interface depth (Figure 3i) associated to a transition to Vs higher than 4.0 km/s (Figure 3j)

3.2 3D Features

We focus on the detection of anisotropy in the middle crust for the three permanent stations. For station CEL in TC our results describe a layer 14 km thick between 9 and 23 km depth, displaying a fast anisotropy axis plunging towards NW, with strength for both P- and S-waves on the order of 5% (Figure 3c). For station MTTG located in IC at the Eastern margin of the Messina Strait, two anisotropic layers have been detected; the first is about 6 km thick at 17 km depth, with a positive symmetry anisotropy axis plunging towards SW, and the second at 23 km depth, having a thickness of 7 km, with a positive anisotropy axis plunging towards

SSE; the estimated amount of anisotropy for these two layers is on the order of 10% for both P- and S-waves (Figure 3h). Station MMME is instead located in Sicily, on the western margin of the Messina Strait, the results obtained for this station are similar to those obtained for MTTG; indeed two layers with anisotropic characteristics have been retrieved, the first is 13 km thick and it's at 8 km depth, displaying about 10% P- and S-wave fast anisotropy plunging towards SW; the second is at 21 km depth and it is 10 km thick with about 10% P- and S-wave fast anisotropy plunging towards SSE (Figure 3k). While the difference in azimuthal direction of the symmetry axes in the two layers is not larger than 40 degrees at MMME, this rotation is robustly resolved by our data, as reported in Figure S16-18.

4. Discussion and Conclusions

The velocity structures and interface distribution at the two sides of the Messina Strait are significantly different. The 1D structure beneath Calabria is extremely variable and changes drastically from the Ionian to the Tyrrhenian side as expected from previous studies [*Piana Agostinetti et al.,* 2009; *Piana Agostinetti and Amato,* 2009].

Under-thrusting of the Ionian domain below Calabria can be seen by the deepening of mantle velocities retrieved beneath the stations (35, 37 and 42 km respectively below Ionian, Central and Tyrrhenian Calabria, Figure 3g,e,b) and may explain low velocity values found at the depth of 30 km and below, beneath CEL (Figures 3b, S2d) ascribed as crustal rocks belonging to the subducted Ionian crust [*Neri et al.,* 2002].

S-velocity models for stations located in Sicily are by far simpler: while stations located in Calabria show relatively complex S-velocity profiles down to a well defined Moho interface, stations located in Sicily show a continuous velocity gradient from the top to the bottom, and almost no clue for a high impedance contrast marking the Moho. The stations located close to Mt Etna (MALI and NOV) and the stations belonging to the IC, show a velocity decrease below 20 km depth; this has a good correspondence to a low velocity layer found in tomographic images by *Monna et al.* [2013], and it's related to Mt. Etna's deep feeding system. Below MMME instead the low velocities in the mid-lower crust are more diffuse, lacking a real inverse velocity jump, as the transition to the mantle does not show a strong Moho interface, rather a slight increase to higher velocities.

Among the three stations for which we were able to model the 3D characteristics of the subsurface structure, the northernmost one, CEL, lies above the slab, relatively far from its edge. Below this station, anisotropy in the crust shows a NW trending fast axis (or, in case of considering slow symmetry axis, a SE trending axis), almost perpendicular to the strike of the subduction trench. A trench-perpendicular anisotropy could indicate the local direction of main subduction processes and it has been also found in the upper mantle in the northern part of the Ionian subduction zone [*Piana Agostinetti et al.,* 2008]. Beneath CEL, the anisotropy is confined between 10 and 20 km, i.e. the lower crust of the Tyrrhenian plate. A positive anisotropy could indicate the presence of aligned minerals (e.g. hornblende, *Meissner et al.* 2006), but we cannot exclude another mechanism for the genesis of the anisotropic behaviour (e.g. ductile deformation, *Ozacar and Zandt*, 2004) driven by extension in the fore-arc crust and facilitated by the high geothermal gradient in the crust, as derived by the high surface heat flow observed along the Tyrrhenian coast [*Davies*, 2013].

Stations MTTG and MMME, on both sides of the Messina Strait, are close to the southern lateral edge of the slab (Figures 1, 3) and show similar anisotropy, for both trend and amount of anisotropy, at similar depths, 10-15 to 30 km. Indeed MTTG located on Calabrian-Ionian coast and MMME located on Sicily display two adjacent anisotropic layers in the middle crust. The shallower layer has a symmetry axis of anisotropy trending SW (or, in case of considering slow symmetry axis, a NE trending axis). The deeper layer displays a symmetry axis of anisotropy trending SSE (NNW in case of slow symmetry axis). Both layers display anisotropy percent as high as 10%. Although the anisotropic characteristics of the media are the same on both sides of the strait, the average S-velocities are not, witnessing a probable different composition of the crust. We cannot exclude that anisotropy beneath the two stations has been generated by two independent processes. However, the strict correspondence between the 3D models for MMME and MTTG, i.e. the thickness of the two anisotropic layers, their depth-position, and the directions of the symmetry axes, suggests a simpler solution involving only one geodynamic process. Due to the different crustal composition beneath the two stations, the mineralogy within the anisotropic layers would be likely different on the two sides of the Messina strait. However, the exact determination of the mineralogy is difficult using RF analysis alone due to the non-uniqueness of the proposed parameterization and it is well beyond the scope of the present study.

Both sites are affected by the presence of the vertical tear fault, that shapes and deforms strongly the area [e.g. *Argnani* 2000; *Govers and Wortel,* 2005]. This particular feature is the

key that suggests that anisotropy across the Messina strait has been generated by the progressive retreat of the Ionian slab and rotation of the Calabrian arc. Calabria and the region of NE Sicily still advance at significant rates of ~ 2-3 mm/yr towards the SE, in response to the SE-ward rollback of the Ionian slab [*D'Agostino et al.,* 2011; *Devoti et al.,* 2011; *Palano et al.,* 2012]. The subducted Ionian domain undergoes slab roll-back, creating lithospheric tears at its edges; tearing takes off at a weaker zone, affecting those crustal layers that are most easily deformable. In our hypothesis, the Messina strait represents the deformation (shear) zone in the overriding plate associated to the tearing process at depth. Its width is about 40 km, from the tear fault location to the tip of Calabria, and it is comparable with the width of the shear zone at mid-crustal depth, suggested for lithospheric faults [*Platt and Behr,* 2011], supporting the presence of similar anisotropic properties (depth, direction and intensity) all across the strait. In fact, the width of such deformation zone is well inside the two end-members explored in *Platt and Behr* (2011), where the minimum ("California wet model)" and maximum ("Dry craton model") width reported are 11 and 156 km, respectively. However, the width of the deformation zone depends on many parameters (e.g. crustal geotherm, mineralogy, water fugacity) and our value should be considered as a soft indication. In any case, our estimate of this parameter is also in agreement with the extension of a deformation zone found in the Northern Apennines [*Rosenbaum and Piana Agostinetti,* 2015; *Piana Agostinetti,* 2015]. The detected anisotropy has to be regarded as a key-feature generated by the opening of the vertical slab tear.

From these observations we can hypothesize that, away from the slab edge (at CEL station), where the trench moves backward, trench-perpendicular anisotropy develops, induced by trench-normal extension. Close to the edge of the slab (at stations MTTG and MMME) a different process explains the anisotropic layers within the crust. The edge acts as a pinch point, between the moving and the stationary plates (the retreating Calabria and the almost locked Sicily), causing the rotation of the tectonic structures there. Hence, the similar vertical succession of anisotropic axes direction at station MTTG and MMME records the progressive rotation of the subducting plate through geological time. The presence of two overlying layers could be linked to the maxima of the rate of trench-retreat in the past. In fact, strong variations in the rate of trench-retreat have been measured during the last 8 Ma, with two well-known maxima in correspondence of the opening of the Vavilov and Marsili basin in the southern Tyrrhenian sea [*Minelli and Faccenna,* 2010]. Present-day rate of trench-retreat is

limited, and the process should be unlikely to overprint the fossil anisotropy developed during phases of vigorous slab rollback and retreat.

The presence of an extended anisotropic zone at mid-crustal depth all across the Messina strait could have important implications for assessing the seismic hazard in the area. In fact, the anisotropic layers represent a somehow weaker zone within the crust, which can potentially limit the depth-extent of the rupture associated to a seismic event. This hypothesis is in agreement with the reconstruction of the fault geometry associated to the 1908 Mw=7.1 Messina event. In fact, a number of models, obtained from different observations, limit the width of the fault plane to 18-20 km, with a top depth generally in the shallow crust at 1-3 km depth (Table 1 in *Cannelli et al.,* [2013]). Moreover, a recent joint analysis of seismological and geodetic data indicates that the rupture propagate from 3 to 12 km depth [*Pino et al.,* 2009]. Thus, the depth of the top of the anisotropic layers almost coincides with the maximum depth of the rupture in the fault models of the Messina event.

Acknowledgments

NPA research has been funded by Science Foundation Ireland projects: 11/SIRG/E2174 and 14/IFB/2742. Waveform data recorded by the RSN (Rete Sismica Nazionale) and ReMo (Rete Mobile) networks are collected by the INGV (Mazza et al., 2012) and made available online at http://eida.rm.ingv.it/ below the IV network code. We thank the Editor J. Ritsema and the two anonymous reviewers whose thorough comments and suggestions improved the quality of our manuscript.

REFERENCES

Ammon, C. J. (1991), The isolation of receiver effects from teleseismic *P* waveforms, Bull. Seismol. Soc. Am., 81, 2504–2510.

Argnani, A. (2000), The Southern Tyrrhenian subduction system: recent evolution and neotectonic implications, Ann. Geophys., 43, 585–607.

Barreca, G., L. Scarfì, F. Cannavò, I. Koulakov, and C. Monaco (2016), New structural and seismological evidence and interpretation of a lithospheric scale shear zone at the southern

edge of the Ionian subduction system (central-eastern Sicily, Italy), Tectonics, 35, 1489–1505 DOI: 10.1002/2015TC004057

Bianchi, I., N. Piana Agostinetti, C. Chiarabba, and P. De Gori (2008), Deep structure of the Colli Albani volcanic district (central Italy) from receiver functions analysis, J. Geophys. Res., 113, B09313, doi: 10.1029/2007JB005548.

Bianchi, I., J. Park, N. Piana Agostinetti, and V. Levin (2010), Mapping seismic anisotropy using harmonic decomposition of receiver functions: An application to Northern Apennines, Italy, J. Geophys. Res., 115, B12317, doi:10.1029/2009JB007061.

Cannelli, V., D. Melini, and A. Piersanti (2013), New insights on the Messina 1908 seismic source from post-seismic sea level change, Geophys. J. Int., 194 (2): 611-622, doi:10.1093/gji/ggt134

Calò, M., C. Dorbath, D. Luzio, S. G. Rotolo, and G. D'Anna (2009), Local earthquake tomography in the Southern Tyrrhenian region of Italy: Geophysical and petrological inferences on the subducting lithosphere, *in* Subduction Zone, Geodynamics, vol. 3, edited by S. Lallemand, and F. Funiciello, pp. 86–100, Springer, Berlin, doi:10.1007/978-3-540-87974.

J. F. Cassidy (1992), Numerical experiments in broadband receiver function analysis, Bull. Seismol. Soc. Am., 82:1453-1474

Cassinis, R., S. Scarascia, and A. Lozej (2003), The deep crustal structure of Italy and surrounding areas from seismic refraction data. A new synthesis, Ital. J. Geosci., 122, 365–376.

Chiarabba, C., P. De Gori, and F. Speranza (2008), The southern Tyrrhenian subduction zone: Deep geometry, magmatism and Plio-Pleistocene evo- lution, Earth Planet. Sci. Lett., 268(1–2), 408–423.

Chiarabba, C., N. P. Agostinetti, and I. Bianchi (2016), Lithospheric fault and kinematic decoupling of the Apennines system across the Pollino range, Geophys. Res. Lett., 43, 3201–3207, *doi:*10.1002/2015GL067610.

D'Agostino, N., E. D'Anastasio, A. Gersavi, I. Guerra, M. R. Nedimovi, L. Seeber, L., and M. S. Steckler (2011), Forearc extension and slow rollback of the Calabrian Arc from GPS measurements, Geophys. Res. Lett., 38: L17304, doi:10.1029/2011GL048270.

Davies, J. H. (2013), Global map of solid Earth surface heat flow, Geochem. Geophys. Geosyst., 14, 4608–4622, doi:10.1002/ggge.20271

Di Bona, M. (1998), Variance estimate in frequency-domain deconvolution for teleseismic receiver function computation, Geophys. J. Int., 134, 634 – 646.

Devoti, R., A. Esposito, G. Pietrantonio, A. R. Pisani, and F. Riguzzi (2011), Evidence of large scale deformation pattern from GPS in the Italian subduction boundary. Earth Planet. Sci. Lett., 230-241, doi:10.1016/j.epsl2011.09.034.

Faccenna, C., T. W. Becker, F. P. Lucente, L. Jolivet, and F. Rossetti (2001), History of subduction and back-arc extension in the Central Mediterranean, Geophys. J. Int., 145: 809-820.

Frederiksen, A. W., and M. G. Bostock (2000), Modeling teleseismic waves in dipping anisotropic structures, Geophys. J. Int., 141, 401 – 412.

Govers, R., and M. J. R. Wortel (2005), Lithosphere tearing at STEP faults: Response to edges of subduction zones, Earth Planet. Sci. Lett., 236, 505–523.

Langston, C.A. (1979), Structure under Mount Rainier, Washington, inferred from teleseismic body waves. J. Geophys. Res. 84, 4749 – 4762.

Levin, V., and J. Park (1998), P–SH conversions in layered media with hexagonally symmetric anisotropy: a cookbook, Pure Appl. Geophys, 151, 669 – 697

Long, M. D., and P. G. Silver (2009), Shear wave splitting and mantle anisotropy: Measurements, interpretations, and new directions, Surv. Geophys., 30, 407–461, doi:10.1007/s10712-009-9075-1.

Lucente, F. P., C. Chiarabba, G. B. Cimini, and D. Giardini (1999), Tomographic constraints on the geodynamic evolution of the Italian region, J. Geophys. Res., 104, 10.1029/1999JB900147.

Lucente, F. P., N. Piana Agostinetti, M. Moro, G. Selvaggi, and M. Di Bona (2005), Possible fault plane in a seismic gap area of the southern Apennines (Italy) revealed by receiver function analysis. J. Geophys. Res., 110, doi: 10.1029/2004JB003187. issn: 0148-0227.

Lucente, F. P., L Margheriti, C. Piromallo, and G. Barruol (2006), Seismic anisotropy reveals the long route of the slab through the western-central Mediterranean mantle, Earth Planet. Sci. Lett., 241, 517–529, doi: 10.1016/j.epsl.2005.10.041

Malinverno, A., and W. B. F. Ryan (1986), Extension in the Tyrrhenian Sea and shortening in the Apennines as result of arc migration driven by sinking of the lithosphere, Tectonics, 5(2), 227–245, *doi:*10.1029/TC005i002p00227.

Margheriti, L. (2008), Understanding Crust Dynamics and Subduction in Southern Italy, Eos Trans. AGU, 89(25), 225–226, doi:10.1029/2008EO250002.

Mazza, S., A. Basili, A. Bono, V. Lauciani, A. G. Mandiello, C. Marcocci, F. Mele, S. Pintore, M. Quintiliani, L. Scognamiglio, and G. Selvaggi (2012). EIDA – Seismic data acquisition, processing, storage and distribution at the National Earthquake Center, INGV, Ann. Geophys. 55, 541-548.

Meissner, R., W. Rabbel, and H. Kern (2006), Seismic lamination and anisotropy of the lower continental crust, Tectonophysics, 416, 81-99

Minelli, L. and C. Faccenna (2010) Evolution of the Calabrian accretionary wedge (central Mediterranean), Tectonics, 29, TC4004, doi:10.1029/2009TC002562

Neri, G., G. Barberi, B. Orecchio, and M. Aloisi (2002), Seismotomography of the crust in the transition zone between the southern Tyrrhenian and Sicilian tectonic domains, Geophys. Res. Lett., 29(23), 2135, doi:10.1029/2002GL015562.

Neri, G., B. Orecchio, C. Totaro, G. Falcone, and D. Presti (2009), Subduction beneath southern Italy close the ending: Results from seismic tomography, Seismol. Res. Lett., 80, 63–70.

Orecchio, B., D. Presti, C. Totaro, and G. Neri (2014), What earthquakes say concerning residual subduction and STEP dynamics in the Calabrian Arc region, south Italy, Geophys. J. Int., 199, 1929–1942.

Ozacar, A. and G. Zandt (2004) Crustal seismic anisotropy in central Tibet: Implications for deformational style and flow in the crust, Geophys. Res. Lett., 31, L23601, doi:10.1029/2004GL021096

Palano, M., L. Ferranti, C. Monaco, M. Mattia, G. Aloisi, V. Bruno, F. Cannavò, and G. Siligato (2012), GPS velocity and strain fields in Sicily and southern Calabria, Italy: Updated geodetic constraints on tectonic block interaction in the central Mediterranean, J. Geophys. Res., 117, B07401, doi:10.1029/2012JB009254.

Piana Agostinetti, N., J. Park, and F. P. Lucente (2008), Mantle Wedge Anisotropy in Southern Tyrrhenian Subduction Zone (Italy), from Receiver Function Analysis, Tectonophisics, 462 (1-4) 35-48, doi:10.1016/j.tecto.2008.03.020

Piana Agostinetti, N., and A. Amato (2009), Moho depth and Vp/Vs ratio in peninsular Italy from teleseismic receiver functions, J. Geophys. Res., 114, B06303, doi:10.1029/2008JB005899.

Piana Agostinetti, N., M. S. Steckler, and F. P. Lucente (2009), Imaging the subducted slab under the Calabrian Arc, Italy, from receiver function analysis, Lithosphere, 1, 131-138, doi:10.1130/L49.1

Piana Agostinetti, N., and A. Malinverno (2010) Receiver Function inversion by trans-

dimensional Monte Carlo sampling, Geophys. J. Int., 181(2) 858–872, doi: 10.1111/j.1365-246X.2010.04530.x

Piana Agostinetti, N. and M. S. Miller (2014), The fate of the downgoing oceanic plate: insight from the northern Cascadia subduction zone, Earth Planet. Sci. Lett., 408, 237–251, doi: 10.1016/j.epsl.2014.10.016.

Piana Agostinetti, N. (2015), The structure of the Moho in the Northern Apennines: Evidence for an incipient slab tear fault?, Tectonophysics, doi:10.1016/j.tecto.2015.05.013

Pino, N. A., A. Piatanesi, G. Valensise, and E. Boschi (2009), The 28 December 1908 Messina Straits earthquake (Mw 7.1): A great earthquake throughout a century of seismology, Seismol. Res. Lett., 80, 243–259, doi:10.1785/gssrl.80.2.243.

Platt, J. P., and W. M. Behr (2011), Deep structure of lithospheric fault zones, Geophys. Res. Lett., 38, *L24308, doi:*10.1029/2011GL049719.

Porter, R., G. Zandt and N. McQuirre (2011) Pervasive lower-crustal seismic anisotropy in Southern California: Evidence for underplated schists and active tectonics, Lithosphere, 3(3), 201-220, doi: 10.1130/L126.1

Rosenbaum, G., and G. S. and Lister (2004), Neogene and Quaternary rollback evolution of the Tyrrhenian Sea, the Apennines, and the Sicilian Maghrebides, Tectonics, 23, TC1013, doi:10.1029/2003TC001518.

Rosenbaum, G., and N. Piana Agostinetti (2015), Crustal and upper mantle response to lithospheric tear faulting: the Livorno-Sillaro Lineament in the northern Apennines, Tectonics, 34, 648–661, doi: 10.1002/2013TC003498

Rovida, A., R. Camassi, P. Gasperini, and M. Stucchi (eds.) (2011),. CPTI11, the 2011 Version of the Parametric Catalogue of Italian Earthquakes (Milano, Bologna, http://emidius.mi. ingv.it/CPTI. http://dx.doi.org/10.6092/INGV.IT-CPTI11).

Sambridge, M. (1999), Geophysical inversion with a neighbourhood algorithm–I. Searching a parameter space, Geophys. J. Int., 138, 479–494, doi:10.1046/j.1365-246X.1999.00876.x.

Savage, M., (1998), Lower crustal anisotropy or dipping boundaries? Effects on receiver functions and a case of study in New Zealand. J. Geophys. Res., 103, 69–87.

Wortel, R., and W. Spakman (2000), Subduction and slab detachment in the Mediterranean-Carpathian region, Science, 290, 1910–1917.

FIGURE CAPTIONS

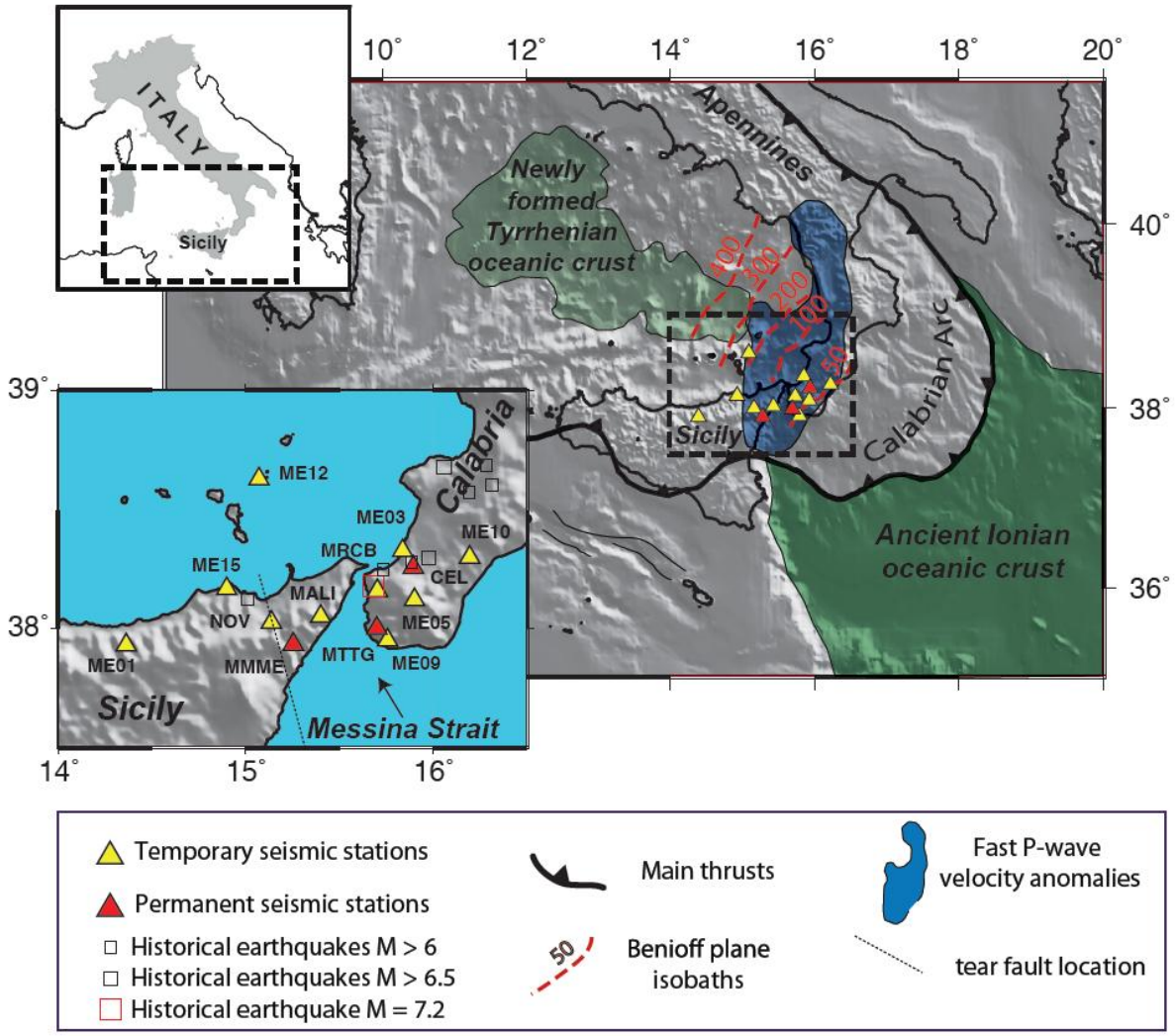

Figure 1: Map of the study area showing the oceanic crust of the Ionian and Tyrrhenian plates. Fast P-wave velocity anomaly from the Calabrian slab is shown as a blue patch, and isobaths of the Benioff plane as red-dashed lines. A close look to the station distribution in the lower left inset, together with the location of the historical earthquakes.

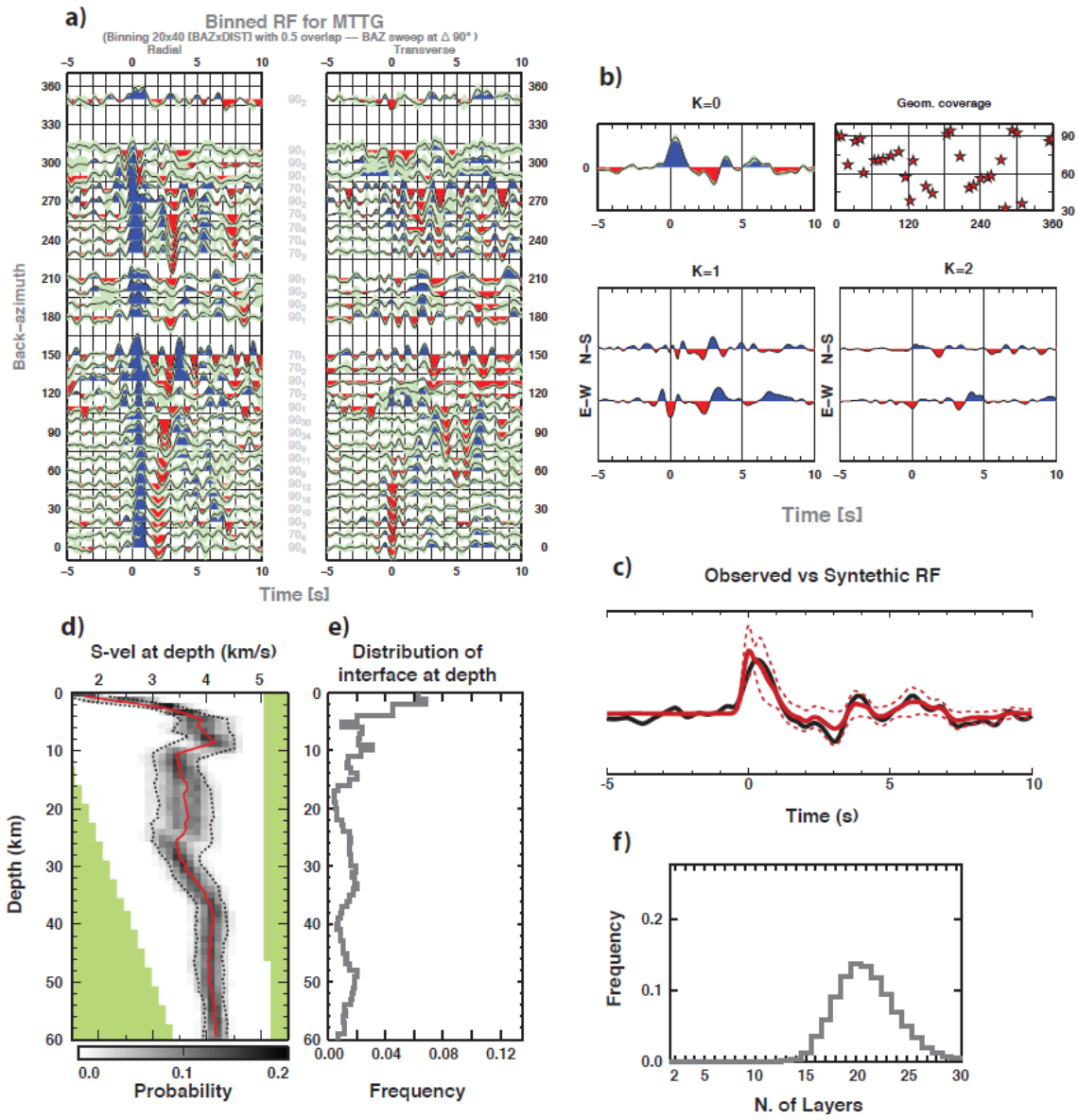

Figure 2: Data and velocity model for station MTTG. a) backazimuthal sweep of Radial (left) and Transverse (right) RF; gray numbers between panels represent bin's Δ, and the number of RF for each bin (subscript). b) Degree 0,1 and 2 of the harmonic decomposition, and epicentral distribution of the teleseisms used, displayed according to backazimuth from North (0°-360°) and Δ (30°-100°). c) Observed vs synthetic k=0 harmonic of the RF. d) Retrieved S-velocity model at depth after the application of the RjMCMC. e) PPD of the interface distribution. f) PPD of the number of layers beneath the station.

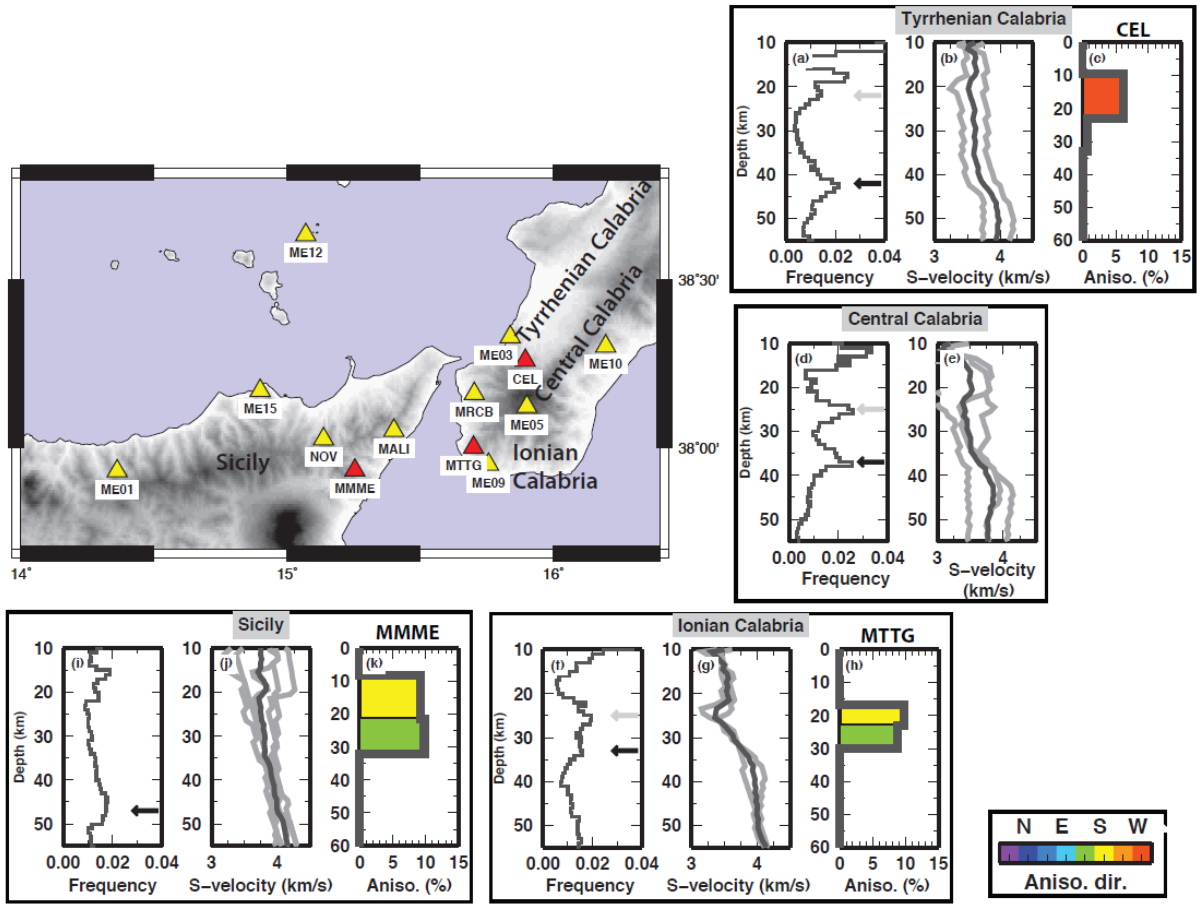

Figure 3: Map of the seismic stations on the background, and groups of seismic stations according to their geographical distribution. Tyrrhenian Calabria: CEL, ME03; Central Calabria: ME05, ME10, MRCB; Ionian Calabria: MTTG, ME09; Sicily: MMME, ME01, NOV, MALI, ME15. For each group three panels are displayed; Left panels: depth-distribution of the interfaces from 1D RjMcMC inversion. The histogram is cumulative over all the inversions for single stations. In Calabria a black (grey) arrow indicates the depth of the Ionian (Tyrrhenian) Moho. In Sicily, a black arrow indicates the depth of the Moho. Central panels: mean posterior S-velocity models from 1D RjMcMC inversion. A black line represents the average between the inversion of the single RF data-set in each region. Grey lines indicate the mean posterior S-velocity models for each single inversion for the stations in the region. Right panels: details of the results of the 3D inversion for 3 stations: CEL (c); MTTG (h); and MMME (k). Each panel reports the percent of anisotropy in the two anisotropic layers. Colors indicate the strike of the symmetry axis in the anisotropic layers.